

Mono and digallium selenide clusters as potential superhalogens

Neelum Seeburrin · Edet F. Archibong ·
Ponnadurai Ramasami

Received: 5 October 2014 / Accepted: 30 November 2014
© Springer-Verlag Berlin Heidelberg 2015

Abstract We present a systematic theoretical study on mono and digallium selenide clusters, Ga_mSe_n ($m=1,2$ and $n=1-4$), along with their negatively and positively charged counterparts. Different theoretical methods, namely density functional theory (DFT), second-order Møller-Plesset perturbation theory (MP2) and coupled cluster singles and doubles, including non-iterative triples [CCSD(T)], were employed in conjunction with the 6-311+G(2df) basis set. The lowest-energy configurations of gallium selenides prefer to be planar, with the exception of cationic GaSe_4 and Ga_2Se_4 . The adiabatic electron affinities (AEA) of Ga_mSe_n ($m=1,2$ and $n=1-4$) clusters range from 1.07 to 3.78 eV, and their adiabatic ionization potentials (AIP) vary from 7.57 to 8.76 eV using the CCSD(T)/B3LYP level of theory. It was found that the AEAs of gallium selenides do not depend solely on the electrophilicity of the clusters but also on their electronic structures. No significant trend was observed in the AIP values and HOMO–LUMO (H–L) gaps with increase in cluster size of the mono and digallium selenide series. Among the dissociation channels, the decomposition of $\text{GaSe}_4 \rightarrow \text{GaSe}_2 + \text{Se}_2$ was found to be thermodynamically most favored. Furthermore, the AEAs of GaSe_2 , GaSe_3 , GaSe_4 and Ga_2Se_4 were found to exceed that of the chlorine atom and are therefore termed as ‘superhalogens’. Finally, the AEAs of the Ga_2X_n ($\text{X}=\text{O–Se}$; $n=2-4$) series were found to be almost similar.

Electronic supplementary material The online version of this article (doi:10.1007/s00894-014-2555-3) contains supplementary material, which is available to authorized users.

N. Seeburrin · P. Ramasami (✉)
Computational Chemistry Group, Department of Chemistry, Faculty of Science, University of Mauritius, Réduit, 80837 Moka, Mauritius
e-mail: p.ramasami@uom.ac.mu

E. F. Archibong
Department of Chemistry and Biochemistry, University of Namibia, Windhoek, Namibia

Keywords Gallium selenides · Electronic structure · Adiabatic electron affinity · Adiabatic ionization potential

Introduction

Gallium chalcogenide clusters have attracted increasing interest owing to their extensive applications ranging from optics to optoelectronics [1–9]. The interaction between gallium and selenium atoms is of utmost importance due to their wide usage in transistors [3], nanophotonic devices, photodetectors [4], memory switching [5] and chalcogenide glasses [6]. GaSe is a potential alternative to graphene for use in tunable nanodevices [7] and as a photocatalyst [8]. In turn, digallium triselenide, Ga_2Se_3 , is a good contender for the passivation of III–V devices [9]. Doped gallium selenide, namely copper indium gallium selenide (CuInGaSe_2), is a leading candidate for photovoltaic devices [10], whereas thallium gallium selenide (TlGaSe_2) is a promising semiconductor for X-ray and γ -ray detectors [11]. Cadmium digallium tetraselenide, CdGa_2Se_4 , is also used in tunable filters and photodetectors [12]. Interestingly, gallium selenide can exist as supertetrahedral clusters and serves as building blocks in the design of novel materials [13].

Substantial research [13–19] has been carried out on supertetrahedral and open framework materials of gallium selenides. These supertetrahedral structures consist of smaller gallium selenide fragments that bind together to form longer chains [13–19]. For instance, an infinite chain of GaSe_2 -PPZ (PPZ=piperazine) consists of smaller units such as GaSe_2^- , GaSe_4^{5-} and $\text{Ga}_6\text{Se}_{14}^{10-}$. GaSe_2 -PPZ could be a potential candidate for semiconductor quantum structures [13]. In the same vein, $\text{Ga}_4\text{Se}_7(\text{en})_2 \cdot (\text{enH})_2$ is built up from two kinds of tetrahedra: GaSe_4 and GaSe_3N [15]. Wu et al. [17] examined zinc gallium selenide supertetrahedral clusters as models for doping. The availability of such a diversity of doped structures has

resulted in a large electronic band gap ranging from 1.5 to 3.4 eV. These tetrahedral clusters can be stabilized via inorganic or organic connectivity leading to hydrid materials that are useful for sensing applications [14, 18].

A wealth of studies has revealed that the stability and electronic properties of clusters can be altered dramatically by changing one atom [20–26]. For example, Ga₂Se is found to adopt a bent configuration [20], unlike Ga₂O, which is linear [21]. Akin to the penta-atomic gallium oxide [22, 23] and sulfide species [24, 25], the ground state geometry of Ga₂Se₃ is V-shaped while Ga₂Se₃[−] is kite shaped using the CCSD(T)//B3LYP/6-311+G(2df) method [26]. With the latter method, the ground state geometry of Ga₃Se₂ is three-dimensional with a C_{2v} symmetry [26], differing from the planar kite geometry of Ga₃O₂ and Ga₃S₂ [22, 24] while Ga₃S₂[−] [25] and Ga₃Se₂[−] prefer a three-dimensional (3D) structure with a D_{3h} symmetry [26]. A decrease in electron affinity is observed when the sulfur atoms of Ga₂S₃ are replaced by selenium atoms, while electron affinity increases when progressing from Ga₃O₂ to Ga₃Se₂ [26]. Analogous to gallium oxides [27, 28], the ground state geometries of neutral and anionic GaS₄ and Ga₂S₄ [29] were found to be kite shaped and a planar D_{2h}, respectively.

Superhalogens are a class of molecules or clusters that have received great attention owing to their high electron affinities [30]. Species whose electron affinities exceed that of chlorine atoms (3.61 eV) [31] are named as superhalogens. In 1981, Gutsev and Boldyrev [32] generalized the formula of a conventional superhalogen as MX_{(n+1)/m} where M is a central metal atom with a valency *n* and X is an electronegative atom with a valency *m*. In this vein, GaO₂, Ga₂O₄ [28] and GaS₂ [29] can be described as ‘superhalogens’. Superhalogens have great potential in the fields of synthesis of unusual organic compounds (e.g., Xe⁺[PtF₆][−]) [33], organic superconductors [32], new dopants [32] and salts with strong oxidizing properties (e.g., KMnO₄) [34].

In view of the above, it has been observed that the substitution of an oxygen or sulfur atom by a selenium atom induces structural and electronic changes in clusters [22, 24–26]. Despite the attention that some gallium selenide clusters have enjoyed [1–9, 13–19, 26], a systematic theoretical investiga-

tion of the proposed gallium selenides, Ga_{*m*}Se_{*n*} (*m*=1,2 and *n*=1–4) has not been undertaken in terms of their structural, vibrational, and electronic properties. Consequently, the objectives of the current theoretical research were to: (1) study the equilibrium structures; (2) provide a reliable theoretical prediction of the relative stabilities, harmonic vibrational frequencies and energetic features such as electron affinities, ionization potentials, HOMO-LUMO (H-L) gaps and dissociation energies (*D_e*); (3) relate the ground state geometries with the oxide and sulfide analogs; and (4) compare the electron affinities of gallium selenide clusters to that of chlorine atom in order to determine whether they can be classified as superhalogens.

Computational methods

Electronic structure computations of mono and digallium selenide; Ga_{*m*}Se_{*n*} (*m*=1,2 and *n*=1–4) clusters were carried out with the Gaussian 09 [35] program by means of the resources provided by GridChem Science Gateway [36–38]. Initial geometries and spin states were taken from isoelectronic gallium oxide and sulfide clusters [21–29] (Figs. 1, 2, 3 and 4). Based on previous investigations on gallium oxide [22, 28] and sulfide [29], the 6-311+G(2df) one-particle basis set was employed. Density functional theory (DFT), namely B3P86, B3PW91 and B3LYP [39–44] and the MP2 [45, 46] level of theory were used. Our previous study on gallium sulfides [29] revealed that the electron affinity of GaS₂ computed with the CCSD(T)//B3LYP approach agrees very well to that obtained at the CCSD(T) level [47]. Therefore, single point computations with the CCSD(T)//B3LYP [44] approximation were used to predict the electronic properties of the clusters reported in this work. In addition, the MOLPRO program [48, 49] was used to optimize the ground state geometries of GaSe at the CCSD(T)/cc-pVTZ level.

The adiabatic electron affinity (AEA), adiabatic electron detachment energy (AEDE), vertical electron detachment energy (VEDE), adiabatic ionization potential (AIP) and vertical ionization potential (VIP) were calculated as follows:

$$\text{AEA} = E(\text{optimized neutral at ground state}) - E(\text{optimized anion at ground state});$$

$$\text{AEDE} = E(\text{optimized corresponding neutral}) - E(\text{optimized anion});$$

$$\text{VEDE} = E(\text{neutral at optimized anion geometry}) - E(\text{optimized anion});$$

$$\text{AIP} = E(\text{optimized cation at ground state}) - E(\text{optimized neutral at ground state});$$

$$\text{VIP} = E(\text{cation at optimized neutral geometry}) - E(\text{optimized cation})$$

The harmonic vibrational frequencies of the optimized geometries were computed to verify the nature of the stationary points. To gain insight into the nature of bonding in the

gallium selenide clusters, natural bond orbital (NBO) analysis [50, 51] was performed with the B3LYP functional. The chemical hardness (η) and HOMO–LUMO (H–L) gaps of

the neutral gallium selenides were calculated with the B3LYP functional. The dissociation energies (D_e) of the studied clusters were determined using the three DFT functionals and the MP2 level of theory.

Results and discussion

Structural properties

Optimized geometrical configurations of the lowest energy states of gallium selenide clusters, Ga_mSe_n ($m=1,2$ and $n=1-4$) are shown in Figs. 1, 2, 3 and 4. The energies of the different isomers relative to the ground state isomers (ΔE) are listed in Table 1. The internal coordinates of the ground state geometries and their corresponding energies are presented in Tables S1–S6. The electronic ground state for neutral GaSe is $^2\Sigma^+$, which is in agreement with experimental observation of GaO [52]. The computations find the most stable electronic states for GaSe^- and GaSe^+ to be $^1\Sigma^+$ and $^3\Sigma^+$ (Fig. 1). This result is consistent with a previous investigation on anionic and cationic GaO [21].

The ground state geometry of neutral GaSe_2 is cyclic with a 2A_2 electronic state (Fig. 2) and is isostructural with GaO_2 [21] and GaS_2 [29]. Akin to GaO_2^- [21] and GaS_2^- [29], anionic GaSe_2 prefers a linear centrosymmetric ($D_{\infty h}$) configuration, which is formed by the Se–Se bond rupture of cyclic GaSe_2 . The first low-lying geometry of GaSe_2 adopts a linear structure while that of GaSe_2^- is bent. On the contrary, GaSe_2^+ is formed by the Ga–Se bond rupture of cyclic GaSe_2 leading to a bent configuration. A linear structure with a Ga–Se–Se arrangement is obtained as the first low lying isomer for GaSe_2^+ . The lowest-energy configuration of neutral and anionic GaSe_3 consists of a diatomic GaSe molecule attached to a Se_2 moiety (Fig. 3), while cationic GaSe_3 prefers a rhombic structure. The first low lying isomer of neutral and anionic GaSe_3 is rhombic whereas that of cationic GaSe_3 has a similar structure to the ground state of GaSe_3 . For GaSe_4 , the kite geometry with a triselenide unit (2B_1) is found to be the lowest-energy structure. The T_d (T1) type structure is found

to converge to the D_{2d} structure. This shows that, although gallium selenide can exist as supertetrahedral, the T1 cluster is unstable in terms of relative energy. The removal of an electron from the anionic GaSe_4 does not affect the lowest-energy configuration of the neutral GaSe_4 as the anion adopts the same structure as the neutral (Fig. 4). Similar ground state geometries were observed for GaO_4 [27] and GaS_4 [29]. Turning to the first low lying isomer, neutral and anionic GaSe_4 prefer the D_{2d} symmetry, which is the lowest-energy structure for GaSe_4^+ . On the other hand, the low lying structure of GaSe_4^+ adopts the kite geometry.

Based on an experimental study, Uy et al. [20] suggested a bent configuration for Ga_2Se . This geometry is in line with our results on neutral Ga_2Se but differs from the ground state geometry of Ga_2O , which was found to be linear [21]. Anionic Ga_2Se adopts a bent structure while cationic Ga_2Se maintains the bent configuration of the neutral ground state geometry, but with a C_s symmetry (Fig. 2). Interestingly, the first low lying isomer of neutral, negatively and positively charged Ga_2Se prefers a linear configuration. For the neutral Ga_2Se_2 series, the L-shaped structure (1A_g) is obtained as the ground state geometry (Fig. 3). Structural differences are observed when comparing the ground state geometries of Ga_2X_2 ($X=\text{O}-\text{Se}$) as Ga_2S_2 is rhombic [29] and Ga_2O_2 is linear [21]. Anionic Ga_2Se_2 is rhombic, formed by closure of the L-shaped structure of Ga_2Se_2 ($^2B_{2u}$), and therefore both gallium atoms have the same charge (Table 2). The structure of Ga_2Se_2^- is analogous to that of Ga_2O_2^- [21] and Ga_2S_2^- [29]. For cationic Ga_2Se_2 , the inner selenium atom receives charge from the two gallium atoms while the terminal selenium atom receives charge only from the inner gallium. This effect is also present in neutral Ga_2Se_2 . The first low lying isomer of neutral and cationic Ga_2Se_2 is rhombic and anionic Ga_2Se_2 adopts a distorted kite structure.

Anionic Ga_2Se_3 [25] and Ga_2Se_3^+ adopt a kite-shape geometry (2B_2) while Ga_2Se_3 prefers a V-shape geometry (1A_1) [25]. A ‘pentagon-like’ structure is obtained as the low-lying isomer of Ga_2Se_3^+ . The lowest-energy structure of neutral and anionic Ga_2Se_4 can be viewed as rhombic with terminal selenium atoms attached to the gallium atoms (D_{2h}) (Fig. 4) with

Fig. 1 Geometrical features of diatomic GaSe with electronic states. Superscripts: *a* B3P86, *b* B3PW91, *c* B3LYP, *d* MP2, *e* CCSD(T)

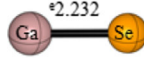
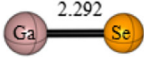
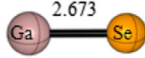
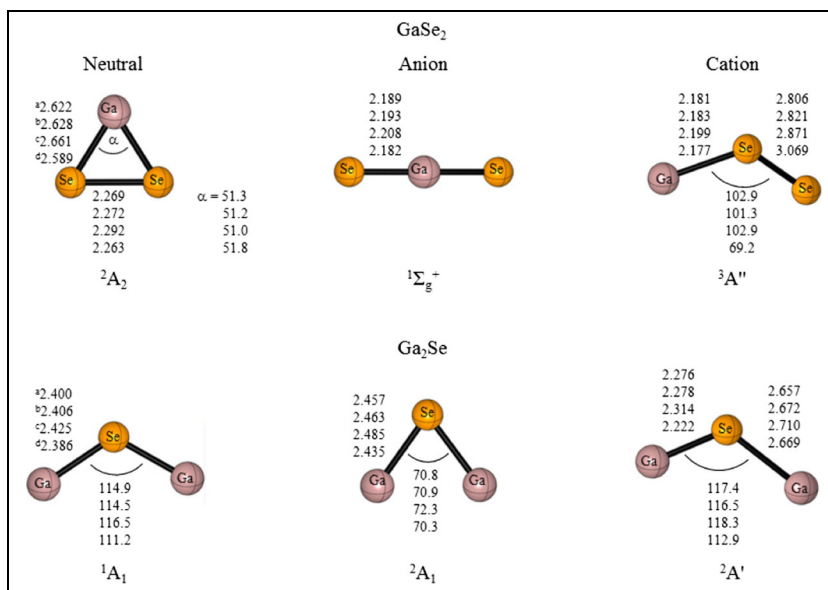
GaSe		
Neutral	Anion	Cation
*2.195	2.261	2.414
*2.198	2.265	2.420
*2.222	2.282	2.478
*2.123	2.247	2.362
*2.232	2.292	2.673
		
$^2\Sigma^+$	$^1\Sigma^+$	$^3\Sigma^+$

Fig. 2 Geometrical features of diatomic GaSe₂ and Ga₂Se with electronic states. Superscripts: *a* B3P86, *b* B3PW91, *c* B3LYP, *d* MP2



³B_{1u} and ²B_{3g} state, respectively. Similar ground state geometry was found for neutral and anionic gallium oxide [28] and sulfide [29]. Like the GaSe₄/GaSe₄⁻ system, it was found that the removal of an electron from the anion Ga₂Se₄ does not affect the lowest-energy configuration of the neutral species. Ga₂Se₄⁺ is formed by the rearrangement of selenium atoms in the planar D_{2h} leading to a ‘fish-like’ structure with a ²A₂ electronic state. In the case of Ga₂Se₄, the low-lying isomer has a ‘fish-like’ structure while that of anionic Ga₂Se₄ prefers a twisted hexagon configuration and cationic Ga₂Se₄ is planar with a D_{2h} symmetry.

To gain insight into the nature of bonding in the gallium selenide clusters, NBO analysis [50, 51] was performed

(Table 2). An interesting feature emerged from the occupation and charge behavior when moving along the neutral and charged series. The charge transfer from gallium to selenium atoms was found to be independent of *n*. The stabilities of the gallium selenide clusters are predominantly governed by heteroatomic Ga–Se bonds over homoatomic Ga–Ga and Se–Se bonds. All the ground state geometries of the neutral, negatively and positively charged GaSe_{*n*} and Ga₂Se_{*n*} prefer planar structures with the exception of cationic mono and digallium tetraselenide. Both cationic GaSe₄ and Ga₂Se₄ are found to have a cyclic moiety. The lowest-energy structures of mono and digallium selenide clusters are shown in Figs. S1 and S2. A structural

Fig. 3 Geometrical features of GaSe₃ and Ga₂Se₂ with electronic states. Superscripts: *a* B3P86, *b* B3PW91, *c* B3LYP, *d* MP2

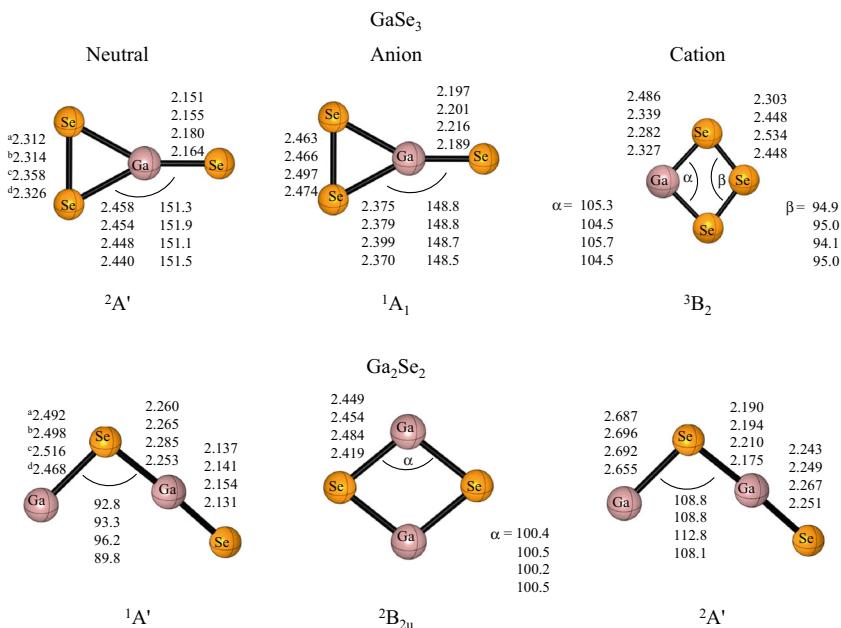
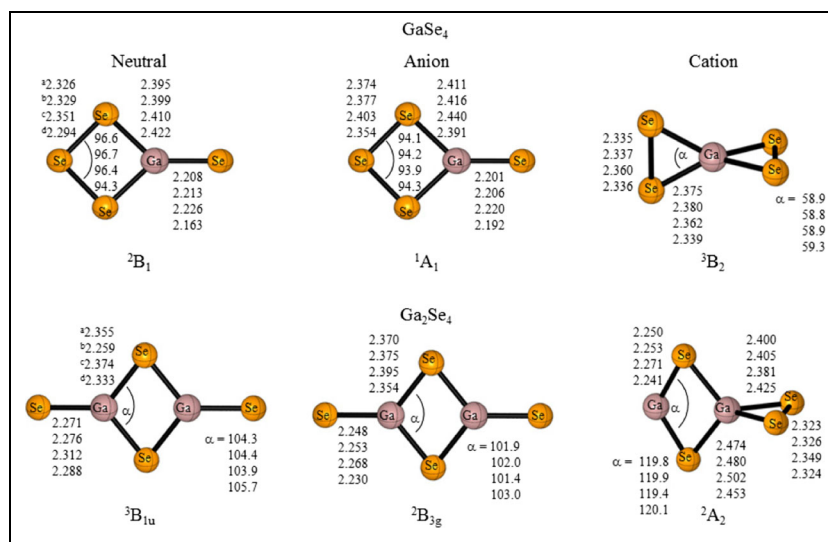


Fig. 4 Geometrical features of GaSe_4 and Ga_2Se_4 with the electronic states. Superscripts: *a* B3P86, *b* B3PW91, *c* B3LYP, *d* MP2



evolution is observed upon addition of a selenium atom to the GaSe_n and Ga_2Se_n series.

Geometrical properties

The geometrical features of the studied gallium selenide clusters, Ga_mSe_n ($m=1,2$ and $n=1-4$) are presented in Figs. 1, 2, 3

Table 1 Energy shifts (eV) of the first low-lying states with respect to ground states of the mono and digallium selenides

Method	B3P86	B3PW91	B3LYP	MP2
GaSe	0.23	0.22	0.15	0.39
GaSe^-	2.39	2.31	2.39	2.45
GaSe^+	0.82	0.85	0.85	0.57
GaSe_2	0.16	0.16	0.17	0.26
GaSe_2^-	1.20	1.21	1.19	1.45
GaSe_3	0.17	0.18	0.21	0.35
GaSe_3^-	1.00	1.00	0.90	1.38
GaSe_3^+	-0.13	-0.11	-0.13	0.18
GaSe_4	0.21	0.19	0.27	0.04
GaSe_4^-	0.30	0.28	0.36	0.18
GaSe_4^+	0.16	0.17	0.09	0.13
Ga_2Se	0.11	0.11	0.09	0.11
Ga_2Se^-	0.55	0.53	0.49	0.54
Ga_2Se^+	1.22	1.22	1.22	1.27
Ga_2Se_2	0.07	0.05	-0.07	0.38
Ga_2Se_2^-	0.50	0.48	0.49	0.58
Ga_2Se_2^+	0.22	0.20	-0.08	0.50
Ga_2Se_3^+	0.07	0.10	0.06	0.44
Ga_2Se_4	0.10	0.12	0.19	0.16
Ga_2Se_4^-	0.24	0.23	0.23	0.33
Ga_2Se_4^+	0.18	0.20	0.11	0.51

and 4. A slight elongation is observed in the monoselenide Ga–Se bond length [0.060 Å with B3LYP/6-311+G(2df) and CCSD(T)/cc-pVTZ] on going from GaSe to GaSe^- . This feature was also observed with GaO [21]. The Ga–Se bond length with CCSD(T)/cc-pVTZ was found to be closer with the B3LYP functional among the three DFT functionals and the MP2 level. In comparison with isoelectronic gallium oxide and sulfide, an increase in the bond angle at the apex; GaO_2 (38.0°) [21], GaS_2 (47.5°) [29] and GaSe_2 (51.0°) [B3LYP] was observed. This feature was attributed to the larger size of selenium atom as compared with oxygen and sulfur atoms. As a consequence, the Se–Se bond length of GaSe_2 was longer than the S–S and O–O bond lengths of GaO_2 and GaS_2 , respectively. Upon removal of an electron from GaSe_2^- , the Se–Ga–Se bond angle compresses from 180.0° to 51.3° (B3P86), 51.2° (B3PW91), 51.0° (B3LYP) and 51.8° (MP2). The bridge Ga–Se bond is elongated whereas the terminal Ga–Se bond is shortened slightly upon removal of an electron from GaSe_3^- (DFT and MP2). In contrast with the GaSe_3 system, the bridge Ga–Se bond is shortened, whereas the terminal Ga–Se bond is elongated slightly upon detachment of an electron from GaSe_4^- (DFT). Furthermore, the Se–Se–Se angle in the rhomboid is smaller in the case of GaSe_4^- . In comparison with GaS_4 [29], the angle between the terminal Ga–Se and neighboring selenium atom of GaSe_4 is smaller by 3.5° and 3.9°, respectively, with the B3LYP functional and MP2 level of theory.

Turning to the Ga_2Se_n series, a compression of the Ga–Se–Ga bond angle was observed (DFT and MP2) from Ga_2Se to Ga_2Se^- . On the other hand, a slight increase in the Ga–Se–Ga bond angle was observed from Ga_2Se to Ga_2Se^+ (DFT and MP2). The B3LYP functional predicts a closer value of the Ga–Se bond length (2.425 Å) of Ga_2Se compared to the reported experimental value (2.6 Å) [20]. The Ga–Se bond length of the anion was slightly longer than that of the neutral

Table 2 Effective natural atomic orbital (NAO) electronic configurations (El.conf) and natural charges [q(M)] of gallium atoms in neutral, negatively and positively charged Ga_mSe_n ($m=1,2$ and $n=1-4$) clusters. All values are in e

	<i>n</i>			
	1	2	3	4
GaSe_n				
El.conf	$4s^{0.70}4p^{0.22}$	$4s^{0.97}4p^{0.29}$	$4s^{0.50}4p^{0.64}6p^{0.01}$	$4s^{0.51}4p^{0.70}$
q (Ga)	0.10	0.23	0.34	0.28
GaSe_n^-				
El.conf	$4s^{1.84}4p^{0.98}$	$4s^{1.02}4p^{1.17}5p^{0.02}$	$4s^{0.98}4p^{1.25}5p^{0.02}$	$4s^{0.99}4p^{1.28}5d^{0.01}6p^{0.02}$
q (Ga)	0.12	0.78	0.75	0.71
GaSe_n^+				
El.conf	$4s^{0.75}4p^{0.07}$	$4s^{0.98}4p^{0.04}$	$4s^{0.63}4p^{0.18}$	$4s^{0.48}4p^{0.78}$
q (Ga)	0.68	0.48	0.69	0.24
Ga_2Se_n				
El.conf	$4s^{1.92}4p^{0.49}$	$4s^{1.95}4p^{0.39}/4s^{1.03}4p^{1.14}$	$4s^{1.04}4p^{1.10}$	$4s^{0.51}4p^{0.69}6p^{0.01}$
q (Ga)	0.58	(0.82, 0.66)	0.84	0.29
Ga_2Se_n^-				
El.conf	$4s^{0.93}4p^{0.30}$	$4s^{0.77}4p^{0.42}$	$4s^{1.42}4p^{1.02}$	$4s^{0.49}4p^{0.65}$
q (Ga)	0.26	0.30	(0.53, 0.15)	0.34
Ga_2Se_n^+				
El.conf	$4s^{0.97}4p^{0.09}/4s^{0.65}4p^{0.12}$	$4s^{0.97}4p^{0.09}/4s^{0.54}4p^{0.50}$	$4s^{0.57}4p^{0.44}/4s^{0.53}4p^{0.66}$	$4s^{0.49}4p^{0.78}/4s^{0.56}4p^{0.44}$
q (Ga)	(0.73, 0.44)	(0.44, 0.46)	(0.49, 0.31)	(0.22, 0.50)

counterpart with DFT and MP2. The Ga–Se bond lengths of neutral and anionic Ga_2Se_2 are in the range 2.131–2.516 Å and 2.419–2.449 Å while that of the cation varies from 2.190 to 2.696 Å (DFT and MP2). The addition of an electron from Ga_2Se_2 leads to an increase in the bond angle at the apex. The bridge Ga–Se bonds of anionic Ga_2Se_4 are slightly longer than the neutral whereas the terminal Ga–Se bonds are shorter (DFT). The bond angle between the terminal Ga–Se and neighboring selenium atom of Ga_2Se_4 is smaller than that reported for Ga_2O_4 [28] and Ga_2S_4 [29]. Unlike the sulfur congener [29], the reported Se–Ga–Se bond angle in the rhomboid of Ga_2Se_4 is smaller when compared with GaSe_4 .

Unlike the Ga_2Se_n series, a general increase in the Se–Se bond length and Se–Ga–Se bond angle was observed when progressing from GaSe_2 to GaSe_4 (DFT and MP2). In all cases, the Ga–Se bond lengths of the neutral gallium selenides were within the range 2.153–2.622 Å (B3P86), 2.158–2.628 Å (B3PW91), 2.180–2.661 Å (B3LYP) and 2.145–2.589 Å (MP2). The Ga–Se bond lengths of the gallium selenides studied are in agreement with those in related gallium selenides such as supertetrahedral zinc gallium selenide (2.369–2.424 Å) [19], $\text{Ba}_3\text{CsGa}_5\text{Se}_{10}\text{Cl}_2$ (2.386–2.411 Å) [19], BaGa_4Se_7 (2.361–2.488 Å) [53] and LiGaSe_2 (2.38–2.40 Å). The Se–Ga–Se bond angle of Ga_2Se_4 is in agreement with those of BaGa_4Se_7 (98.8–126.2°) [53] and LiGaSe_2 (106.7–109.6°) [54].

Vibrational properties

The harmonic vibrational frequencies of the lowest-energy states of the gallium selenide clusters are presented in Tables S1–S6 (Supporting Information). All the ground state geometries of the studied gallium selenide clusters were found to have no imaginary frequencies. The stretching frequency of GaSe and GaSe^- were almost same whereas a lower frequency value is reported for GaSe^+ . The frequency computations of neutral Ga_2Se were lower compared to the experimental values obtained by Uy et al. [13] (345, 302 and 132 cm^{-1}) with the three DFT functionals and MP2 level of theory. An analysis of the modes of vibration of GaSe_2 indicates that the highest frequency mode corresponds to the stretching of the Se–Se bond. The lowest frequency mode of cationic GaSe_2^+ indicates that the diatomic GaSe is weakly attached to the terminal selenium atom. This feature is further confirmed by Mulliken charges as the charge on the selenium atom is almost negligible ($-0.001e$). Comparison with available experimental data reveals that the Se_2 frequency value (430, 404 and 426 cm^{-1}) [55] is smaller than the Se–Se stretching of GaSe_2 (460 cm^{-1}) and larger than the Se–Se stretching of anionic GaSe_3 (255 cm^{-1}), cationic GaSe_4 (310 cm^{-1}) and Ga_2Se_4 (342 cm^{-1}), respectively. Furthermore, the stretching of terminal Ga–Se bond of

neutral and cationic GaSe₃ is larger than that reported for GaSe and GaSe⁺. No significant trend was observed in the frequency values upon sequential addition of selenium atoms for both the GaSe_n and Ga₂Se_n series.

Electronic properties

Adiabatic electron affinities

The AEAs of gallium selenide clusters are given in Table 3 and the HOMO plots are shown in Figs. 5 and 6. It should be noted that the HOMO of the anionic clusters is represented by two colors (red and green) that corresponds to negative and positive isosurface, respectively. The ground state electronic configuration of GaSe₂⁻ is (12π_g)²(12π_u)²(10σ_u)²(10σ_g)²(4δ_g)²(2δ_u)². The excess electron in the anion is distributed over both selenium atoms (Fig. 5). The AEA is 4.12 eV (B3P86), 3.57 eV (B3PW91), 3.52 eV (B3LYP), 3.90 eV (MP2) and 3.78 eV [CCSD(T)//B3LYP], respectively. The electronic configuration of GaSe₃⁻ is (29a₁)²(19b₂)²(12b₁)²(7a₂)². The excess electron of GaSe₃⁻ is localized on the terminal selenium atom as shown in Fig. 5. The electronic configuration of the GaSe₄⁻ ground state is (37a₁)²(23b₂)²(16b₁)²(8a₂)². Akin to GaSe₃⁻, the excess electron of GaSe₄⁻ is localized on the terminal selenium atom (Fig. 5). The AEAs are in the range of 3.46–4.11 eV. Turning to the Ga₂Se_n series, Ga₂Se⁻ has an electronic configuration of (21a₁)¹(15b₂)²(8b₁)²(5a₂)². The transition ¹A₁ (C_{2v})+e⁻←²A₁ (C_{2v}) involves the removal of an electron from the 21a₁ molecular orbital (MO) to yield the ¹A₁ (C_{2v}) ground state of Ga₂Se. The lowest-lying doublet state of Ga₂Se₂⁻ has an electronic configuration of (17a_g)²(12b_{1u})²(12b_{2u})¹(7b_{3u})²(7b_{3g})²(5b_{2g})²(4b_{1g})²(2a_u)² and the AEA varies from 1.92 (MP2) to 2.89 eV (B3P86). The electronic configuration of anionic Ga₂Se₄ is (25a_g)²(20b_{1u})²(16b_{2u})²(11b_{3u})²(11b_{3g})¹(8b_{2g})²(6b_{1g})²(3a_u)². The extra electron of Ga₂Se₄⁻ is evidently seen around the terminal selenium atoms (Fig. 6). The calculated AEA falls within 3.80–4.38 eV according to the DFT functionals whereas for MP2 and CCSD(T)//B3LYP, the AEA ranges from 3.62 to

3.66 eV. With the exception of GaSe₂ and Ga₂Se₂, the AEDEs and AEAs are the same for the clusters because of the similar ground state geometry of the neutral and the anionic species.

By analogy with gallium oxides [21] and sulfides [22], a significant increase in the AEA values is observed when progressing from Ga₂Se to Ga₂Se₄ (Fig. 7). A plausible explanation for this trend is that clusters with excess of selenium atoms are electrophilic and thereby present higher electron affinity values. Similar increase in the AEAs is expected for the GaSe_n series but instead, a decrease in the electron affinity values is observed for GaSe₃ and GaSe₄ (Fig. 9). This clearly shows that the AEAs of these gallium selenides are not related only to the total number of selenium atoms but also to their electronic structures. Among the gallium selenides studied, Ga₂Se₄ has the highest electron affinity at all levels of theory employed. As mentioned earlier, the extra electron of both anionic GaSe₂ and Ga₂Se₄ is distributed over the selenium atoms, thereby explaining their high electron affinities (Fig. 5).

Out of the eight gallium selenide clusters considered, the electron affinities of four species, namely GaSe₂, GaSe₃, GaSe₄ and Ga₂Se₄, exceed the electron affinities of chlorine atoms (3.62 eV) [30] and can be termed as superhalogens. Only GaSe₂ is found to satisfy the superhalogen formula and can be described as a conventional superhalogen. A close inspection of the AEAs of digallium chalcogenides (Ga₂X_n; X=O–Se and n=2–4) [21, 22, 24, 26, 28, 29] reveals that their AEA values are almost similar, with Ga₂S₄ having the highest electron affinity.

Ionization potentials

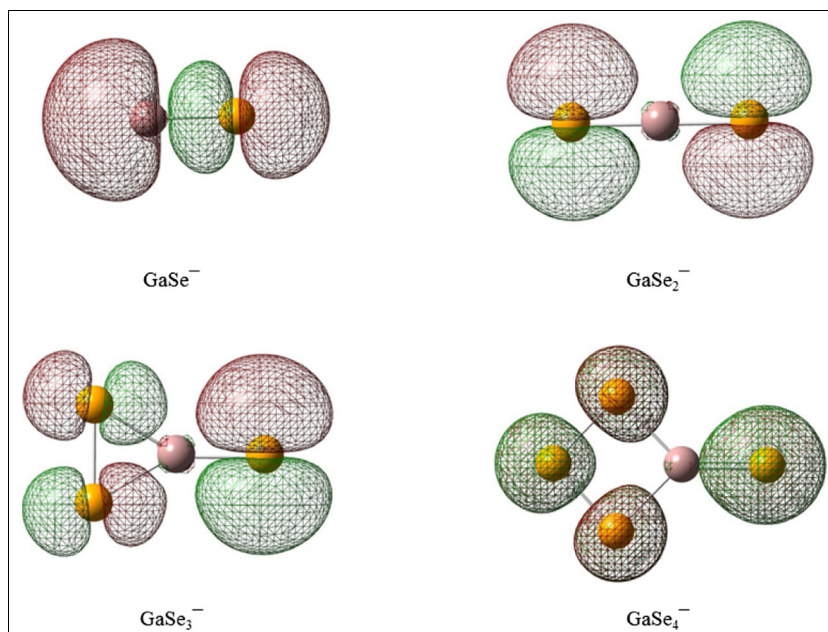
The AIP of gallium selenide clusters are given in Table 4. The calculated AIP of GaSe was compared with the literature value. The calculated AIP of GaSe is 9.40 eV (B3P86), 8.81 eV (B3PW91), 8.78 eV (B3LYP), 8.85 eV (MP2), 8.76 eV [CCSD(T)//B3LYP] and 9.28 eV [CCSD(T)/cc-pVTZ]. Among the different levels of theory employed, the AIP value of GaSe with the B3P86 functional (9.40 eV) yields a closer value when compared with the experimental data (AIP of GaSe: 11.2±0.3 eV). The AIPs of GaSe₂ are in the range of 8.00–8.70 eV whereas that of GaSe₃ ranges from 7.89 (B3LYP) to 9.14 eV (MP2). Furthermore, the AIP of GaSe₄ varies from 7.56 (MP2) to 8.35 eV (B3P86). On the other hand, the AIP of Ga₂Se is reported to be 8.53 eV (B3P86), 7.95 eV (B3PW91 and B3LYP), 7.92 eV (MP2), 7.94 eV [CCSD(T)//B3LYP] and 7.81 eV [CCSD(T)/cc-pVTZ]. Here, the CCSD(T) value obtained with the MOLPRO program (Table 4) is found to be closer to the experimental value (AIP of Ga₂Se: 7.4±0.3 eV [20]). The AIPs of Ga₂Se₂ are in the range of 7.93–8.52 eV whereas that of Ga₂Se₃ ranges from 7.72 [CCSD(T)//B3LYP] to 8.37 eV (B3P86). The AIP of Ga₂Se₄ varies from 7.53 (MP2) to

Table 3 Adiabatic electron affinities (AEAs) of the gallium selenide clusters using different levels of theory

Cluster	B3P86	B3PW91	B3LYP	MP2	CCSD(T)//B3LYP
GaSe	3.25	2.69	2.73	2.66	2.43 (2.47) ^a
GaSe ₂	4.12	3.57	3.52	3.90	3.78
GaSe ₃	4.13	3.57	3.56	3.65	3.62
GaSe ₄	4.01	3.46	3.46	3.69	3.63
Ga ₂ Se	1.66	1.13	1.00	1.03	1.07
Ga ₂ Se ₂	2.89	2.35	2.40	1.92	2.12
Ga ₂ Se ₄	4.38	3.80	3.84	3.62	3.63

^a Value obtained from CCSD(T)/cc-pVTZ level

Fig. 5 Orbital accommodating the excess electron of anionic monogallium selenides



8.07 eV (B3P86). As shown in Fig. 8, irregular patterns of AIPs are observed for GaSe_n and Ga_2Se_n ($n=1-4$) series.

HOMO–LUMO (H–L) gaps

The HOMO–LUMO (H–L) gaps for neutral gallium selenide clusters are presented in Fig. 9. The H–L gaps for the lowest-energy configurations vary from 3.29 (GaSe_4) to 4.87 eV (Ga_2Se_4) with the B3LYP functional. A large value of the H–L energy gap is related to enhance chemical stability [56]. Therefore, the sufficiently large H–L gaps

ensure the stability of these gallium selenide clusters. For the GaSe_n series, a general decrease in the H–L gaps was observed with an increase in the selenium-to-metal ratio. Similar observations are found for the energy gap values from Ga_2O_4 [28] to Ga_2Se_4 . This feature can be attributed to the extra mixing of orbitals in gallium selenides compared to the oxides. The value obtained for the H–L gap of GaSe seems to be unrealistic when compared with the bandgap of GaSe as the bulk value is 0.995 eV and a value of 2.352 eV is obtained for GaSe monolayer [1]. The H–L gaps of GaSe_3 , GaSe_4 and Ga_2Se_2 are in good agreement

Fig. 6 Orbital accommodating the excess electron of anionic digallium selenides

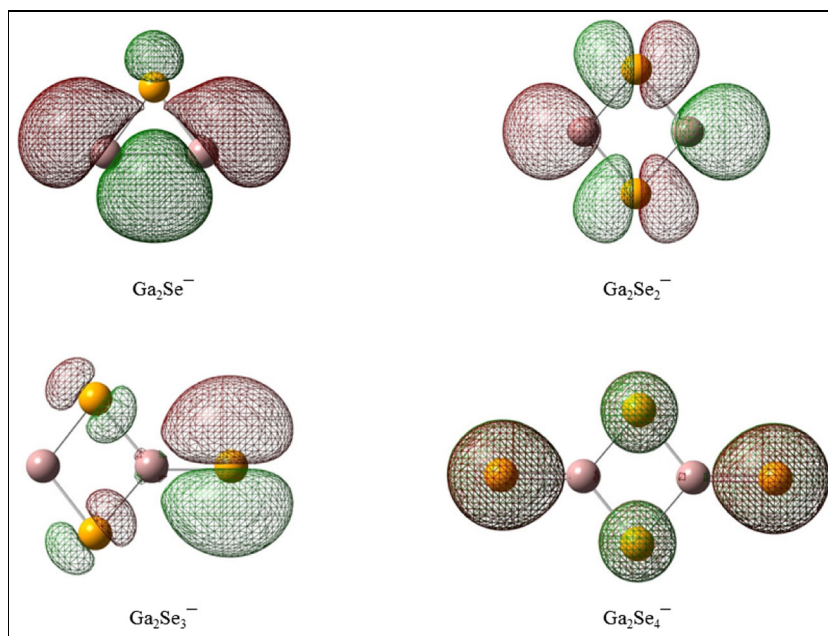
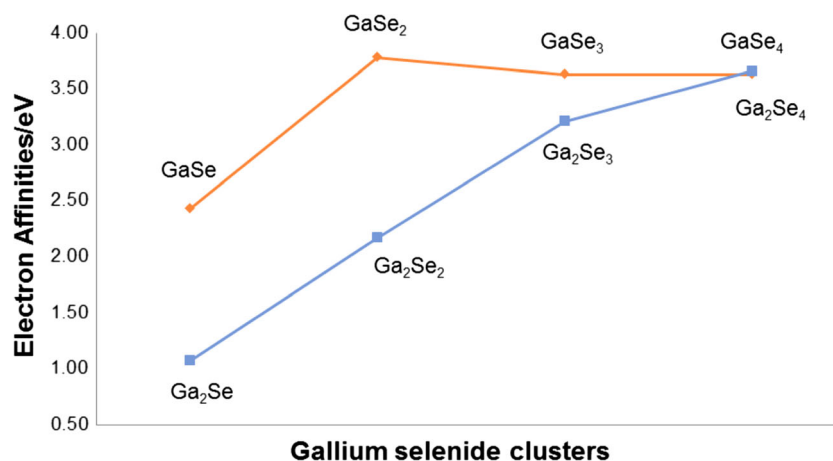


Fig. 7 Electron affinities of the gallium selenide clusters at CCSD(T)//B3LYP level



with the experimental bandgaps of undoped ZnGaSe and doped ZnGaSeS [17]. In addition, no correlation is observed between the H–L gaps and the AEAs or AIPs.

Chemical hardness (η)

The maximum hardness principle, suggested by Pearson states: ‘Molecules arrange their electronic structure so as to have the maximum possible hardness’ [57]. The chemical hardness (η) of the gallium selenides with the B3LYP functional is listed in Table S7. Chemical hardness is expressed as:

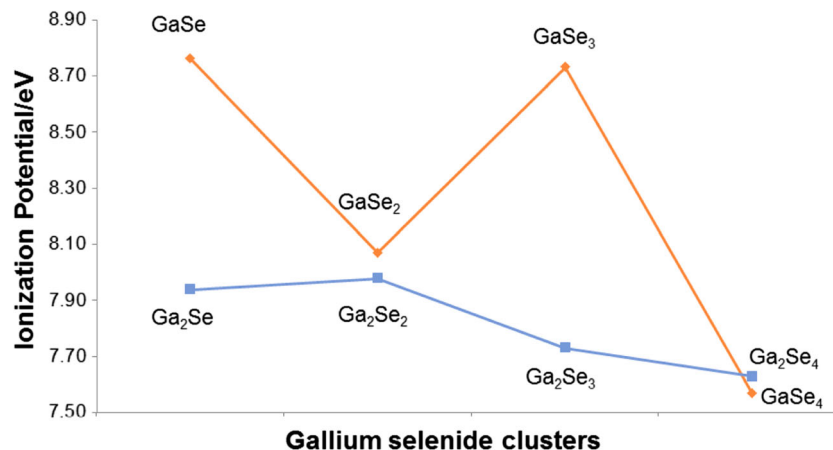
$$\eta \approx (\text{VIP} - \text{VEDE}) / 2$$

A decrease in the selenium-to-metal ratio increases the chemical hardness of the Ga₂Se_{*n*} clusters. The H–L gaps of clusters can be related to hardness (η). Clusters with small H–L gaps are said to be ‘soft’ and more polarizable [58]. As mentioned earlier, the H–L gaps for the studied gallium selenides are large and therefore can be considered as ‘hard’ clusters.

Thermodynamic stability

To estimate the thermodynamic stability of the neutral species, the energies of decay through channels corresponding to the release of selenium atom, selenium molecule and triselenide moiety were calculated and presented in Table 5. These energies were obtained as the difference in total energies of the initial state and the sum of total energies of the decay fragments. The dissociation energy (D_e) of GaSe into its constituent elements was calculated to be 337.6 (B3P86), 325.8 (B3PW91), 316.7 (B3LYP) and 337.5 (MP2) kJ mol⁻¹, respectively. The values obtained with the B3PW91 and B3LYP functionals are in agreement with the available experimental data (256–326 kJ mol⁻¹) [13]. With the exception of GaSe, the monogallium selenides were found to initiate a cascade release of selenium molecule that is thermodynamically stable with respect to Se₂ loss. No significant trend was observed through the channels of decay for digallium selenides. The GaSe₄ → GaSe₂ + Se₂ decomposition was found to be thermodynamically most favored and the Ga₂Se → 2Ga + Se is the least preferred toward

Fig. 8 Ionization potentials of the gallium selenide clusters at CCSD(T)//B3LYP level



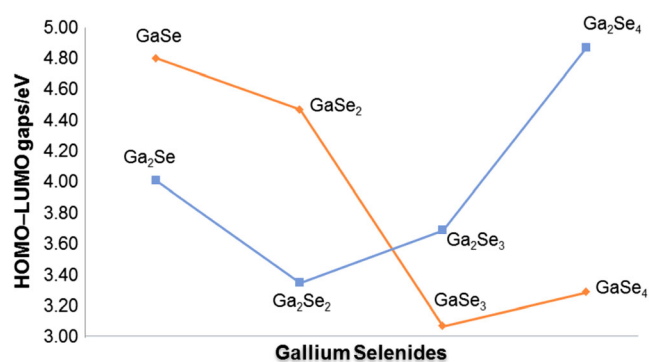


Fig. 9 HOMO–LUMO (H–L) gaps of the gallium selenide clusters with the B3LYP functional

dissociation. In the case of the GaSe_3 cluster, formation of the Se_2 molecule is favored upon dissociation. This behavior can be explained due to the fact that the terminal selenium atom of the Ga–Se bond is cleaved easily as its atomic charge is less negative. This behavior was also observed for neutral Ga_2Se_n ($n=2-4$). In contrast to the gallium oxide [21], but akin to gallium sulfide analogue [22], the dissociation of digallium tetraselenide yields Ga_2Se_2 and a Se_2 molecule.

Table 5 Dissociation energies (D_e , kJ mol^{-1}) of gallium selenides through different channels

Channels	B3P86	B3PW91	B3LYP	MP2
$\text{GaSe} \rightarrow \text{Ga} + \text{Se}$	337.6	325.8	316.7	337.5
$\text{GaSe}_2 \rightarrow \text{Ga} + \text{Se}_2$	277.8	268.5	257.1	286.6
$\text{GaSe}_2 \rightarrow \text{GaSe} + \text{Se}$	312.4	301.9	293.4	291.5
$\text{GaSe}_2 \rightarrow \text{Ga} + 2\text{Se}$	650.0	627.7	610.1	629.0
$\text{GaSe}_3 \rightarrow \text{GaSe} + \text{Se}_2$	172.6	165.8	144.2	206.2
$\text{GaSe}_3 \rightarrow \text{GaSe}_2 + \text{Se}$	232.4	223.2	203.7	257.2
$\text{GaSe}_3 \rightarrow \text{GaSe} + 2\text{Se}$	544.8	525.0	497.1	548.7
$\text{GaSe}_4 \rightarrow \text{GaSe}_2 + \text{Se}_2$	150.4	142.2	118.4	183.5
$\text{GaSe}_4 \rightarrow \text{GaSe} + \text{Se}_3$	250.5	243.0	227.0	260.2
$\text{GaSe}_4 \rightarrow \text{GaSe}_3 + \text{Se}$	290.2	278.3	267.7	274.1
$\text{GaSe}_4 \rightarrow \text{Ga} + 2\text{Se}_2$	428.2	410.7	375.5	470.0
$\text{Ga}_2\text{Se} \rightarrow \text{GaSe} + \text{Ga}$	328.6	319.5	318.5	332.0
$\text{Ga}_2\text{Se} \rightarrow 2\text{Ga} + \text{Se}$	666.2	645.3	635.2	669.5
$\text{Ga}_2\text{Se}_2 \rightarrow 2\text{GaSe}$	292.8	283.8	268.7	349.8
$\text{Ga}_2\text{Se}_2 \rightarrow \text{Ga}_2\text{Se} + \text{Se}$	301.9	290.1	266.9	355.3
$\text{Ga}_2\text{Se}_2 \rightarrow \text{GaSe}_2 + \text{Ga}$	318.0	307.8	291.9	395.8
$\text{Ga}_2\text{Se}_3 \rightarrow \text{Ga}_2\text{Se} + \text{Se}_2$	187.9	181.7	151.5	264.4
$\text{Ga}_2\text{Se}_3 \rightarrow \text{GaSe} + \text{GaSe}_2$	238.8	232.8	212.8	309.8
$\text{Ga}_2\text{Se}_3 \rightarrow \text{Ga}_2\text{Se}_2 + \text{Se}$	258.3	250.8	237.6	251.5
$\text{Ga}_2\text{Se}_3 \rightarrow \text{Ga}_2\text{Se} + 2\text{Se}$	560.2	541.0	504.5	606.8
$\text{Ga}_2\text{Se}_4 \rightarrow \text{Ga}_2\text{Se}_2 + \text{Se}_2$	165.7	163.4	133.3	187.9
$\text{Ga}_2\text{Se}_4 \rightarrow 2\text{GaSe}_2$	206.0	202.8	168.1	297.2
$\text{Ga}_2\text{Se}_4 \rightarrow \text{GaSe}_3 + \text{GaSe}$	286.0	281.4	257.6	331.5
$\text{Ga}_2\text{Se}_4 \rightarrow \text{Ga}_2\text{Se}_3 + \text{Se}$	279.6	271.8	248.8	277.9
$\text{Ga}_2\text{Se}_4 \rightarrow \text{Ga}_2\text{Se}_2 + 2\text{Se}$	538.0	522.7	486.3	530.4

Table 4 Adiabatic ionization potential (AIPs) of gallium selenide clusters using different levels of theory

Cluster	B3P86	B3PW91	B3LYP	MP2	CCSD(T)//B3LYP
GaSe	9.40	8.81	8.78	8.85	8.76 (9.28) ^a
GaSe_2	8.70	8.11	8.00	8.14	8.07
GaSe_3	8.46	7.90	7.89	8.27	8.73
GaSe_4	8.35	7.76	7.85	7.56	7.57
Ga_2Se	8.53	7.95	7.95	7.92	7.94
Ga_2Se_2	8.52	7.93	8.04	8.12	7.98
Ga_2Se_3	8.37	7.78	7.93	7.81	7.72
Ga_2Se_4	8.07	7.53	7.61	7.40	7.56

^a Value obtained from CCSD(T)/cc-pVTZ level

Conclusions

The structural and electronic properties of a series of neutral, negatively and positively charged gallium selenide Ga_mSe_n ($m=1,2$ and $n=1-4$) clusters were examined using theoretical methods. In most cases, the lowest energy structures of the gallium selenide clusters are planar with heteroatomic Ga–Se bonds. A structural evolution was observed upon sequential addition of a selenium atom to the GaSe_n and Ga_2Se_n series.

The Ga–Se bond lengths, Se–Ga–Se bond angles, AIP values, H–L gaps and D_c are in agreement with literature values. Furthermore, it was found that the AEAs of the gallium selenides do not depend solely on electrophilicity but also on their electronic structures. The electron affinities of GaSe₂, GaSe₃, GaSe₄ and Ga₂Se₄ exceed that of chlorine atoms and therefore are termed as ‘superhalogens’. In this vein, GaSe₂, GaSe₃, GaSe₄ and Ga₂Se₄ clusters hold great potential as building blocks for the development of new materials. The results of this research can open the door to a rich structural variety of gallium selenide clusters and a diversity of bonding angles that might lead to novel electronic properties.

Acknowledgments N.S. acknowledges support from the Mauritius Tertiary Education Commission (TEC). The authors also acknowledge facilities at the University of Mauritius and the University of Namibia. The authors would like to thank the anonymous reviewers for useful comments to improve the manuscript.

References

1. Lei S, Ge L, Liu Z, Najmaei S, Shi G, You G, Lou J, Vajtai R, Ajayan PM (2013) *Nano Lett* 13:2777–2781
2. Leontiev I, Evtodiev I, Nedeff V, Stamate M, Caraman M (2009) *Appl Phys Lett* 94:071903–071903-3
3. Late DJ, Liu B, Luo J, Yan A, Matte HSSR, Grayson M, Rao CNR, Dravid VP (2012) *Adv Mater* 24:3549–3554
4. Hu PA, Wen ZZ, Wang LF, Tan PH, Xiao K (2012) *ACS Nano* 6: 5988–5994
5. Zhang YF, Wang R, Kang ZH, Qu LL, Jiang Y, Gao JY, Andreev YM, Lanski GV, Kokh KA, Morozov AN, Shaiduko AV, Zuev VV (2011) *Opt Commun* 284:1677–1681
6. Gujar TP, Shinde VR, Park JW, Lee HK, Jung KD, Joo OS (2008) 54: 829–834
7. Ma Y, Dai Y, Guo M, Yu L, Huang B (2013) *Phys Chem Phys* 15: 7098–7105
8. Zhuang HL, Hennig RG (2013) *Chem Mater* 25:3235–3238
9. Tang G, Yang Z, Luo L, Chen W (2008) *J Alloy Compd* 459:472–476
10. Harvey TB, Mori I, Stolle CJ, Bogart TD, Ostrowski DP, Glaz MS, Du J, Pernik DR, Akhavan VA, Kesrouani H, Vanden Bout DA, Korgel BA (2013) *ACS Appl Mater Interfaces* 5:9134–9140
11. Johnsen S, Liu Z, Peters JA, Song JH, Peter SC, Malliakas CD, Cho NK, Jin H, Freeman AJ, Wessels BW, Kanatzidis MG (2011) *Chem Mater* 23:3120–3128
12. Joshi NV, Luengo J, Vera F (2007) *Mater Lett* 61:1926–1928
13. Bu X, Zheng N, Wang X, Wang B, Feng P (2004) *Angew Chem Int Ed* 43:1502–1505
14. Mao A, Aitken BG, Youngman RE, Kaseman CD, Sen S (2013) *J Phys Chem B* 117:16594–16601
15. Vaqueiro P (2010) *Dalton Trans* 39:5965–5972
16. Xu G, Guo P, Song S, Zhang H, Wang C (2009) *Inorg Chem* 48: 4628–4630
17. Wu T, Bu X, Zhao X, Khazhakyann R, Feng P (2011) *J Am Chem Soc* 133:9616–9626
18. Dong Y, Peng Q, Wang R, Li Y (2003) *Inorg Chem* 42:1794–1796
19. Yu P, Zhou LJ, Chen L (2012) *J Am Chem Soc* 134:2227–2235
20. Uy OM, Muenow DW, Ficalora PJ, Margrave JL (1968) *Trans Faraday Soc* 64:2998–3005
21. Gowtham S, Costales A, Pandey R (2004) *J Phys Chem B* 108: 17295–17300
22. Archibong EF, Mvula EN (2005) *Chem Phys Lett* 408:371–376
23. Gowtham S, Deshpande M, Costales A, Pandey R (2005) *J Phys Chem B* 109:14836–14844
24. Seeburrin N, Archibong EF, Ramasami P (2008) *Chem Phys Lett* 467:23–27
25. BelBruno JJ, Sanville E, Burnin A, Muhangi AK, Maluyutin A (2009) *Chem Phys Lett* 478:132–138
26. Seeburrin N, Abdallah HH, Archibong EF, Ramasami P (2011) *Eur Phys J D* 63:351–358
27. Archibong EF, Ramasami P (2011) *Comput Theor Chem* 964:324–328
28. Seeburrin N, Abdallah HH, Ramasami P (2012) *J Phys Chem A* 116: 3215–3223
29. Seeburrin N, Abdallah HH, Archibong EF, Ramasami P (2014) *Struc Chem* 25:755–766
30. Gutsev GL, Boldyrev AI (1981) *Chem Phys* 56:277–283
31. Hotop H, Lineberger WC (1985) *J Phys Chem Ref Data* 14:731–750
32. Gutsev GL, Boldyrev AI (1981) *Chem Phys Lett* 84:352–355
33. Bartlett N (1962) *Proc Chem Soc* 6:218–218
34. Gutsev GL, Rao BK, Jena P, Wang XB, Wang LS (1999) *Chem Phys Lett* 312:598–605
35. Frisch MJ, Trucks GW, Schlegel HB, Scuseria GE, Robb MA, Cheeseman JR, Montgomery JA Jr, Vreven T, Kudin KN, Burant JC, Millam JM, Iyengar SS, Tomasi J, Barone V, Mennucci B, Cossi M, Scalmani G, Rega N, Petersson GA, Nakatsuji H, Hada M, Ehara M, Toyota K, Fukuda R, Hasegawa J, Ishida M, Nakajima T, Honda Y, Kitao O, Nakai H, Klene M, Li X, Knox JE, Hratchian HP, Cross JB, Bakken V, Adamo C, Jaramillo J, Gomperts R, Stratmann RE, Yazyev O, Austin AJ, Cammi R, Pomelli C, Ochterski J, Ayala PY, Morokuma K, Voth GA, Salvador P, Dannenberg JJ, Zakrzewski VG, Dapprich S, Daniels AD, Strain MC, Farkas O, Malick DK, Rabuck AD, Raghavachari K, Foresman JB, Ortiz JV, Cui Q, Baboul AG, Clifford S, Cioslowski J, Stefanov BB, Liu G, Liashenko A, Piskorz P, Komaromi I, Martin RL, Fox DJ, Keith T, Al-Laham MA, Peng CY, Nanayakkara A, Challacombe M, Gill PMW, Johnson BG, Chen W, Wong MW, Gonzalez C, Pople JA (2009) *Gaussian 09, Revision D.01*, Gaussian Inc, Wallingford
36. Dooley R, Milfeld K, Guiang C, Pamidighantam S, Allen GJ (2006) *J Grid Comput* 4:195–208
37. Milfeld K, Guiang C, Pamidighantam S, Giuliani J (2005) *Proceedings of the 2005 Linux Clusters: The HPC Revolution*. Linux Clusters Institute, Urbana, IL
38. Dooley R, Allen G, Pamidighantam S (2005) *Proceedings of the 13th annual Mardi Gras Conference Louisiana State University, Baton Rouge, LA*
39. Perdew JP (1986) *Phys Rev B* 33:8822–8824
40. Perdew JP (1986) *Phys Rev B* 34:7406
41. Perdew JP, Wang Y (1992) *Phys Rev B* 45:13244–13249
42. Perdew JP, Chevary JA, Vosko SH, Jackson KA, Pederson MR, Singh DJ, Fiolhais C (1992) *Phys Rev B* 46:6671–6687
43. Lee C, Yang W, Parr RG (1988) *Phys Rev B* 37:785–788
44. Becke AD (1993) *J Chem Phys* 98:5648–5652
45. Bartlett RJ (1981) *Ann Rev Phys Chem* 32:359–402
46. Hehre WJ, Radom L, Schleyer PR, Pople JA (1986) *Ab initio molecular orbital theory*. Wiley, New York
47. Raghavachari K, Trucks GW, Pople JA, Head-Gordon M (1989) *Chem Phys Lett* 157:479–483
48. Werner HJ, Knowles PJ, Knizia G, Manby FR, Schütz M (2012) *Comput Mol Sci* 2:242–253
49. Werner HJ, Knowles PJ, Knizia G, Manby FR, Schütz M, Celani P, Korona T, Lindh R, Mitrushenkov A, Rauhut G, Shamasundar KR, Adler TB, Amos RD, Bernhardsson A, Berning A, Cooper DL, Deegan MJO, Dobbyn AJ, Eckert F, Goll E, Hampel C, Hesselmann A, Hetzer G, Hrenar T, Jansen G, Köppl C, Liu Y, Lloyd AW, Mata RA, May AJ, McNicholas SJ, Meyer W, Mura ME, Nicklaß A, O’Neill DP, Palmieri P, Peng D, Pflüger K, Pitzer

- R, Reiher M, Shiozaki T, Stoll H, Stone AJ, Tarroni R, Thorsteinsson T, Wang M MOLPRO, version 2012.1, a package of ab initio programs
50. Reed AE, Weinstock RB, Weinhold F (1985) *J Chem Phys* 83:735–746
 51. Reed AE, Curtiss LA, Weinhold F (1988) *Chem Rev* 88:899–926
 52. Meloni G, Sheehan SM, Neumark DM (2005) *J Chem Phys* 122:074317-1-7
 53. Yao JY, Mei DJ, Bai L, Lin ZS, Yin WL, Fu PZ, Wu YC (2010) *Inorg Chem* 49:9212–9216
 54. Isaenko L, Yelisseyev A, Lobanov S, Titov A, Petrov V, Zondy JJ, Krinitsin P, Merkulov A, Vedenyapin V, Smirnova J (2003) *Cryst Res Technol* 38:379–387
 55. Barrow RF, Burton WG, Callomon JH (1970) *J Chem Soc Faraday Trans* 66:2685–2693
 56. Zhong MM, Kuang XY, Wang ZH, Shao P, Ding LP (2013) *J Mol Model* 19:263–274
 57. Pearson RG (1997) *Chemical hardness: applications from molecules to solids*. Wiley-VCH, Weinheim
 58. Parr RG, Chattaraj PK (1991) *J Am Chem Soc* 113:1854–1855